Journal of Sound and Vibration (1997) **199**(2), 323–336

DISSIPATION OF WAVE ENERGY IN A VISCOELASTIC JUNCTION BETWEEN ELASTIC BARS: DEPENDENCE ON TRANSMISSION DIRECTION

T. Nygren and B. Lundberg

School of Engineering, *Uppsala University*, *Box* 534, *S*-751 21 *Uppsala*, *Sweden*

and

L.-E. Andersson

Department of Mathematics, *Linköping University*, *S*-581 83 *Linköping*, *Sweden*

(*Received* 16 *October* 1995, *and in final form* 3 *June* 1996)

Dissipation, reflection and transmission of an incident extensional wave and its energy at a non-uniform viscoelastic junction between two equal and collinear elastic bars are considered. In particular, the dependence of the energy dissipation, reflection and transmission coefficients on the transmission direction has been studied theoretically and experimentally. With the use of a 1-D linear model it is shown that the dissipated energy, and the reflected wave and its energy, generally depend on the transmission direction, while in contrast, the transmitted wave and its energy, as a manifestation of reciprocity, do not. Significant differences between the dissipated energies, and between the reflected waves and their energies, for the two transmission directions were obtained experimentally for four non-symmetric junctions. Good agreements were obtained between the corresponding transmitted waves and their energies for the two transmission directions. The bars used in the experimental tests were made of steel, and the junctions consisted of segments of polypropylene, high density polyethylene and polymethyl methacryalate between end segments of aluminium. For a junction made of polymethyl methacryalate and aluminium, numerical simulations were carried out and fair agreement was obtained with the experimental results.

1. INTRODUCTION

The ability of elastic waves to carry energy is used in several engineering applications. In percussive drilling, e.g., compressional waves carry energy from the impacted end of a drill string to a drill bit, where a substantial part of the wave energy is used to crush the rock. On the way to the drill bit, the waves are commonly transmitted through joints, where some of their energy is reflected and some is dissipated. Similarly, when a structure of any kind is impacted, waves are generated and transmitted to other parts of the structure where they are sometimes of use and sometimes detrimental. On their way through the structure, the waves are usually transmitted through junctions of different kinds. In these, some of the wave energy is reflected and some is commonly dissipated due to friction or material damping. Clearly, the properties of a junction with regard to dissipation, reflection and transmission are often of importance.

Wave transmission through viscoelastic junctions were studied, e.g., by Mao and Rader [1] and by Hanneman and Kinra [2, 3]. Energy aspects were considered for elastic junctions

0022–460X/97/020323 + 14 $25.00/0/sv960616

between elastic bars by Lundberg *et al*. [4] and for viscoelastic junctions between such bars by Nygren *et al*. [5]. In these studies, the shape of the incident wave was optimized for maximum energy transmission. Other related work for elastic junctions between elastic bars was carried out by Andersson and Lundberg [6], who showed that for a given elastic junction with a certain distribution of characteristic impedance Z, there are generally a number of different junctions which have the same transmission properties as the original one. If the characteristic impedances of the input and output bars are the same (Z_0), one of these junctions can be obtained by reversion of the characteristic impedance function, which corresponds to changing the transmission direction similarly as in this paper. Two other such junctions can be obtained by inversion (i.e., replacing the characteristic impedance Z by Z_0^2/Z), and by combined inversion and reversion, of the characteristic impedance function. Generally, however, the operation of inversion is not meaningful for a viscoelastic junction with complex characteristic impedance.

This paper is concerned with the dissipation, reflection and transmission of an incident extensional wave and its energy at a non-uniform viscoelastic junction between two equal and collinear elastic bars. In particular, the dependence of the energy dissipation, reflection and transmission coefficients on the transmission direction (or junction orientation) is studied theoretically and experimentally. Naturally, the theoretical results can be interpreted for similar systems (e.g., a non-uniform viscoelastic layer between elastic media).

With the aid of a 1-D linear model, it will be demonstrated that the dissipated energy, and the reflected wave and its energy, generally depend on the transmission direction. In contrast, it will be seen that the transmitted wave and its energy have no directional dependence. This manifestation of reciprocity was demonstrated for similar systems by, e.g., Mace [7] and Allard *et al*. [8]. Thus, the dissipated energy, and the reflected wave and its energy, generally change if the junction is reversed, whereas the transmitted wave and its energy do not.

The differences between the dissipated energies, and between the reflected waves and their energies, for the two transmission directions will be studied experimentally for five different junctions, four non-symmetric and one symmetric, between steel bars. Similarly, the degree to which there is agreement between the corresponding transmitted waves and their energies for the two transmission directions will be studied. The junctions used in the experimental tests were made from segments of polypropylene, high density polyethylene and polymethyl methacryalate between end segments of aluminium.

2. THEORY

Consider a non-uniform viscoelastic junction between two equal and collinear elastic bars as illustrated in Figure 1. The junction has characteristic impedance Z and wave speed c which are complex functions of the radian frequency ω and the axial co-ordinate x. These quantities are defined by $Z = A\sqrt{E\rho}$ and $c = \sqrt{E/\rho}$, where $A = A(x)$ is the cross-sectional area, $E = E(x, \omega)$ is the complex modulus, and $\rho = \rho(x)$ is the density. The bars have characteristic impedance Z_0 and wave speed c_0 which are real and constant, and defined correspondingly. Normal forces associated with elastic waves travelling in the directions of increasing and decreasing x are denoted by f_1^p and f_1^n, respectively, at the end of the first bar and f_2^p and f_2^n, respectively, at the beginning of the second bar.

The propagation of viscoelastic waves in the junction is assumed to be governed by the 1-D linear relations

$$\partial \hat{f}/\partial x = \mathrm{i}\omega A\rho\hat{v}, \qquad \partial \hat{v}/\partial x = \mathrm{i}\omega \hat{f}/AE, \tag{1}$$

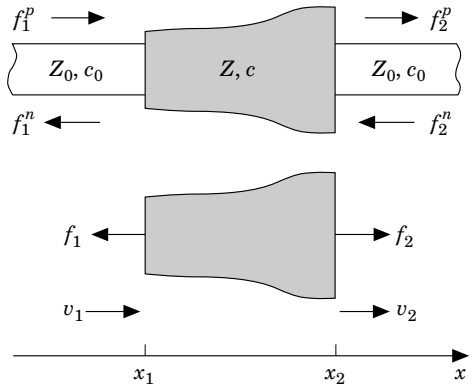

Figure 1. Non-uniform viscoelastic junction between equal and collinear elastic bars.

where $f(x, t)$ is normal force, positive in tension, and $v(x, t)$ is particle velocity, positive in the direction of increasing x, and t is time. The quantities $\hat{f}(x, \omega)$ and $\hat{v}(x, \omega)$ are Fourier transforms, i.e., $\hat{f}(x, \omega) = \int_{-\infty}^{\infty} f(x, t)\, \mathrm{e}^{-\mathrm{i}\omega t}\, \mathrm{d}t$, and similarly for v. The first of equations (1) is the equation of motion and the second follows from the relations $\partial v/\partial x = \partial \varepsilon/\partial t$ and $\hat{f} = AE\hat{\varepsilon}$, where ε is the strain. They can be rewritten as

$$\partial \hat{\mathbf{s}}/\partial x = \gamma \mathbf{Q}\hat{\mathbf{s}}, \tag{2}$$

where

$$\hat{\mathbf{s}} = \begin{bmatrix} \hat{f} \\ \hat{v} \end{bmatrix}, \qquad \mathbf{Q} = \begin{bmatrix} 0 & Z \\ 1/Z & 0 \end{bmatrix} \tag{3}$$

are a state vector and a system matrix, respectively, and $\gamma = \mathrm{i}\omega/c$.

From equation (2) one can obtain the linear relation

$$\hat{\mathbf{s}}_1 = \mathbf{P}\hat{\mathbf{s}}_2 \tag{4}$$

between the state vectors

$$\hat{\mathbf{s}}_1 = \begin{bmatrix} \hat{f}_1 \\ \hat{v}_1 \end{bmatrix}, \qquad \hat{\mathbf{s}}_2 = \begin{bmatrix} \hat{f}_2 \\ \hat{v}_2 \end{bmatrix}, \tag{5}$$

at the first and second ends of the junction.

The determinant of the transfer matrix $\mathbf{P}$ is related to the system matrix $\mathbf{Q}$ through [9]

$$\det(\mathbf{P}) = \exp\left[-\int_{x_1}^{x_2} \mathrm{trace}(\gamma \mathbf{Q})\, \mathrm{d}x \right]. \tag{6}$$

From this relation and the second of equations (3) it follows that

$$\det(\mathbf{P}) = 1, \tag{7}$$

which expresses the reciprocity of the junction.

The relation (4) between the state vectors $\hat{\mathbf{s}}_1$ and $\hat{\mathbf{s}}_2$ can be transformed into the relations $\hat{\mathbf{f}} = \mathbf{Z}\hat{\mathbf{v}}$ and $\hat{\mathbf{v}} = \mathbf{Y}\hat{\mathbf{f}}$ between the force vector $\hat{\mathbf{f}} = [\hat{f}_1, \hat{f}_2]^{\mathrm{T}}$ and the velocity vector

$\hat{\mathbf{v}} = [-\hat{v}_1, \hat{v}_2]^{\mathrm{T}}$. In these relations $\mathbf{Z}$ and $\mathbf{Y} = \mathbf{Z}^{-1}$ are the impedance and mobility matrices, respectively. From relation (7) it follows that these matrices are symmetric, i.e.,

$$\mathbf{Z}^{\mathrm{T}} = \mathbf{Z}, \qquad \mathbf{Y}^{\mathrm{T}} = \mathbf{Y}, \tag{8}$$

which is another way of expressing the reciprocity of the junction.

The state vectors $\hat{\mathbf{s}}_1$ and $\hat{\mathbf{s}}_2$ can be expressed in terms of the wave vectors

$$\hat{\mathbf{w}}_1 = \begin{bmatrix} \hat{f}_1^p \\ \hat{f}_1^n \end{bmatrix}, \qquad \hat{\mathbf{w}}_2 = \begin{bmatrix} \hat{f}_2^p \\ \hat{f}_2^n \end{bmatrix}, \tag{9}$$

through the relations

$$\hat{\mathbf{s}}_1 = \mathbf{R}\hat{\mathbf{w}}_1, \qquad \hat{\mathbf{s}}_2 = \mathbf{R}\hat{\mathbf{w}}_2, \tag{10}$$

where

$$\mathbf{R} = \begin{bmatrix} 1 & 1 \\ -1/Z_0 & 1/Z_0 \end{bmatrix}. \tag{11}$$

Substituting relations (10) into (4), one obtains $\mathbf{R}\hat{\mathbf{w}}_1 = \mathbf{P}\mathbf{R}\hat{\mathbf{w}}_2$ and hence

$$\hat{\mathbf{w}}_1 = \mathbf{H}\hat{\mathbf{w}}_2, \tag{12}$$

where $\mathbf{H} = \mathbf{R}^{-1}\mathbf{P}\mathbf{R}$ is the wave matrix. From relation (7) and $\det(\mathbf{R}^{-1}) = 1/\det(\mathbf{R})$ it follows that this matrix, similarly as $\mathbf{P}$, has the property

$$\det(\mathbf{H}) = 1, \tag{13}$$

which is still another way of expressing the reciprocity of the junction.

Consider now wave transmission through the junction, first in one direction, and then in the other. If the direction of wave transmission is from the first into the second bar (superscript A), the reflected and transmitted waves can be obtained from equations (12) and (13) as

$$\hat{f}_R^A = (H_{21}/H_{11})\hat{f}_I, \qquad \hat{f}_T^A = (1/H_{11})\hat{f}_I, \tag{14}$$

respectively, where $\hat{f}_I$ is the incident wave. If the direction of transmission is opposite (superscript B), there is the corresponding result

$$\hat{f}_R^B = (-H_{12}/H_{11})\hat{f}_I, \qquad \hat{f}_T^B = (1/H_{11})\hat{f}_I. \tag{15}$$

Thus, the transmitted waves are the same for the two transmission directions,

$$\hat{f}_T^A = \hat{f}_T^B, \tag{16}$$

whereas the reflected waves are generally different. This manifestation of reciprocity is illustrated in Figure 2.

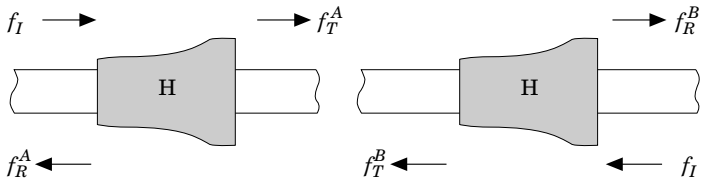

Figure 2. The property $\det(\mathbf{H}) = 1$ of the wave matrix $\mathbf{H}$ implies $f_T^A = f_T^B$ as a manifestation of reciprocity.

The energies of the incident, reflected and transmitted waves are

$$W_I = (1/Z_0)\int_{-\infty}^{\infty} f_I^2 \,\mathrm{d}t, \quad W_R = (1/Z_0)\int_{-\infty}^{\infty} f_R^2 \,\mathrm{d}t, \quad W_T = (1/Z_0)\int_{-\infty}^{\infty} f_T^2 \,\mathrm{d}t, \tag{17}$$

while the energy dissipated in the junction can be expressed as the difference between the energy of the incident wave and that of the reflected and transmitted waves together, i.e.,

$$W_D = W_I - (W_T + W_R) \tag{18}$$

(superscripts A or B omitted).

The energy reflection and transmission coefficients are

$$\eta_R^A = W_R^A/W_I = \int_{-\infty}^{\infty} |H_{21}/H_{11}|^2 |\hat{f}_I|^2 \,\mathrm{d}\omega \Big/ \int_{-\infty}^{\infty} |\hat{f}_I|^2 \,\mathrm{d}\omega,$$

$$\eta_T^A = W_T^A/W_I = \int_{-\infty}^{\infty} |1/H_{11}|^2 |\hat{f}_I|^2 \,\mathrm{d}\omega \Big/ \int_{-\infty}^{\infty} |\hat{f}_I|^2 \,\mathrm{d}\omega \tag{19}$$

for transmission direction A and

$$\eta_R^B = W_R^B/W_I = \int_{-\infty}^{\infty} |H_{12}/H_{11}|^2 |\hat{f}_I|^2 \,\mathrm{d}\omega \Big/ \int_{-\infty}^{\infty} |\hat{f}_I|^2 \,\mathrm{d}\omega,$$

$$\eta_T^B = W_T^B/W_I = \int_{-\infty}^{\infty} |1/H_{11}|^2 |\hat{f}_I|^2 \,\mathrm{d}\omega \Big/ \int_{-\infty}^{\infty} |\hat{f}_I|^2 \,\mathrm{d}\omega \tag{20}$$

for transmission direction B. In these relations, use has been made of equations (14), (15) and (17), and of Parseval's relation. Similarly, the energy dissipation coefficients are

$$\eta_D^A = 1 - (\eta_T^A + \eta_R^A) \quad \text{and} \quad \eta_D^B = 1 - (\eta_T^B + \eta_R^B), \tag{21, 22}$$

respectively.

From relations (19) and (20) it follows that

$$\eta_T^A = \eta_T^B, \tag{23}$$

i.e., the energy transmission coefficients are the same in the two cases, whereas the energy reflection coefficients η_R^A and η_R^B are generally different. From these results and relations (21) and (22), it follows that the energy dissipation coefficients η_D^A and η_D^B are also generally different.

3. EXPERIMENT AND SIMULATION

The experimental set-up used is illustrated in Figure 3.

A cylindrical hammer with length L_H was accelerated to the velocity V by means of an air gun. It impacted an input bar with length 4035 mm which was connected to an output bar with length 3385 mm through a junction. Each bar was guided by five low-friction slide bearings (only two are shown in the figure) so that they were free to move axially during the tests. A damping device at the end of the output bar served to absorb the energy and stop the motion after a test.

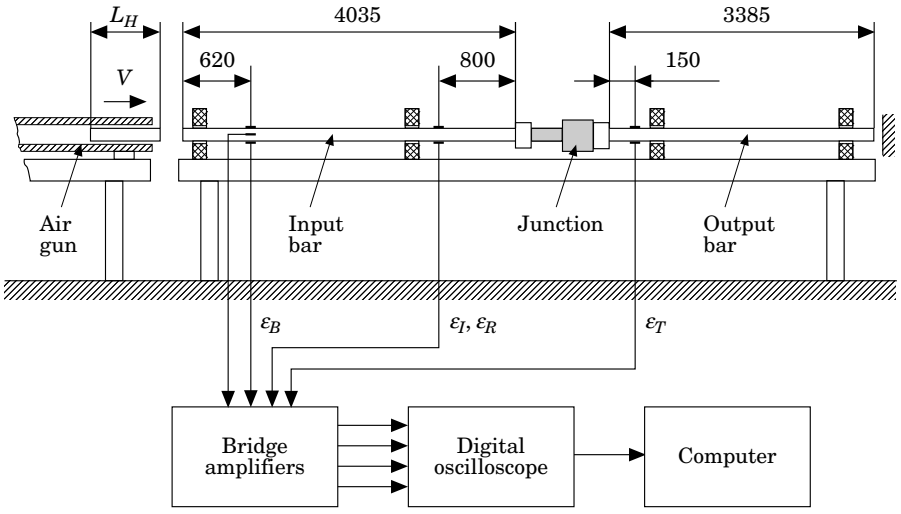

Figure 3. Experimental set-up. Dimensions in mm.

The hammer and the bars were made of steel and had the same diameter 15 mm. Therefore, under the nearly 1-D conditions which prevailed, an approximately rectangular incident wave was generated in the input bar. With good accuracy, the length of this wave was $2L_H$, and its strain amplitude was $(1/2)V/c_0$. The length of the incident wave was varied in the range of 200 to 800 mm by using seven hammers with lengths 100, 150, 200, . . . , 400 mm, and the strain amplitude was kept at a level of 80 ± 5 micro-strain by using an impact velocity around 0·8 m/s. This level was considered to be sufficiently low to assure a linear response of the junctions, and sufficiently high to produce low-noise signals from axial strain gauges on the input and output bars.

A pair of diametrically opposite strain gauges (Micro Measurements CEA-06-125UN-120) was attached to the input bar at a distance of 800 mm from the junction in order to measure the strains $\varepsilon_I(t)$ and $\varepsilon_R(t)$ associated with the incident and reflected waves separated from each other, and from waves reflected from the impacted end. A similar pair of strain gauges was attached to the output bar at a distance of 150 mm from the junction in order to measure the strain $\varepsilon_T(t)$ associated with the transmitted wave separated from waves reflected from the far end. The gauges of each pair were connected to a bridge amplifier (Measurement Group 2210) in opposite branches, so that contributions from small accidental bending strains were suppressed.

One horizontal and one vertical pair of diametrically opposite strain gauges (Micro Measurements EA-06-120LZ-120) were mounted 620 mm from the impacted end of the input bar in order to monitor the absence of significant bending strain $\varepsilon_B(t)$, i.e., the quality of impact. The gauges of each pair were connected to a bridge amplifier (Measurement Group 2210) in neighbouring branches so that contributions from axi-symmetric strains were suppressed.

Shunt calibration was used, and the strain signals were recorded by means of a four-channel digital oscilloscope (Nicolet Pro 20) with a sampling interval of 1 μs. The recorded signals were transferred to a computer for evaluation of the energy reflection and transmission coefficients as

$$\eta_R = \int \varepsilon_R^2(t)\,\mathrm{d}t \Big/ \int \varepsilon_I^2(t)\,\mathrm{d}t, \qquad \eta_T = \int \varepsilon_T^2(t)\,\mathrm{d}t \Big/ \int \varepsilon_I^2(t)\,\mathrm{d}t \tag{24}$$

(superscripts A or B omitted) and of energy dissipation coefficients according to relations (21) and (22).

The five different junctions labelled J1 to J5 and shown in Figure 4 were used in the tests. Each junction consisted of four or five collinear cylindrical segments of different lengths, diameters and materials. The two end segments had length 25 mm and diameter 30 mm, and were made of aluminium (Al). The intermediate segments had lengths 30, 45 or 60 mm and diameters 25, 30 or 45 mm, and were made of polypropylene (PP), high density polyethylene (PE) or polymethyl methacryalate (PMMA). Segments of different materials were glued together using Loctite 406. Before the glue was added, the surfaces of polypropylene and polyethylene were treated with Loctite 770 polyolefin primer. As shown in Figure 5, the junctions were connected to the input and output bars by means

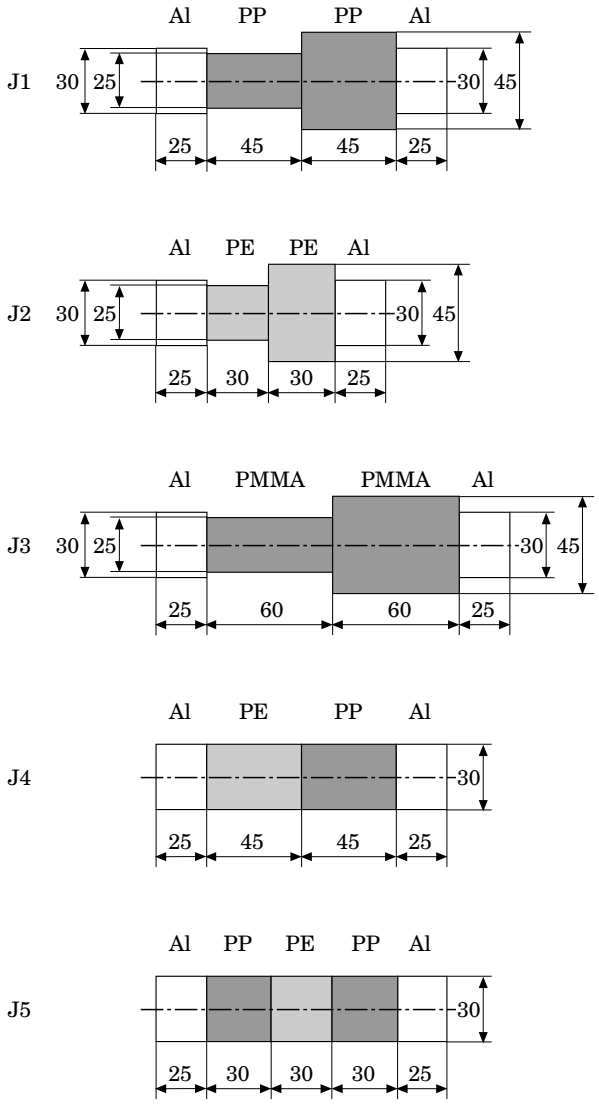

Figure 4. Junctions used in the tests. J1 to J3 are non-symmetric due to geometry, J4 is non-symmetric due to materials, and J5 is symmetric. Dimensions in mm.

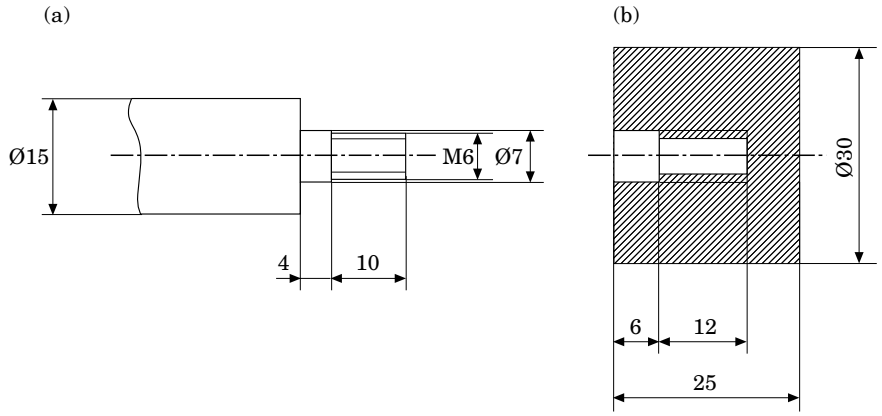

Figure 5. Connection between (a) end of steel bar and (b) aluminium end segment of junction. Dimensions in mm.

of partially threaded taps at the ends of the steel bars, which were screwed into partially threaded holes in the aluminium end segments of the junctions. The inner parts of the taps and the outer parts of the holes, which were free from threads, served to provide centricity.

For each combination of the five junctions, and the seven hammers, two series of five tests each were carried out, i.e., altogether 350 tests. In the first series, labelled A, the left end of each junction, as they are shown in Figure 4, was connected to the input bar, while the right end was connected to the output bar. Thus, the transmission direction A was from left to right in the figure. In the second series, labelled B, the junctions were reversed. For each series of five tests, average values and standard deviations were determined for the energy dissipation, reflection and transmission coefficients.

For the junction J3, made of PMMA and aluminium, the reflection and transmission of waves were simulated, so that numerical values were obtained for the energy dissipation, reflection and transmission coefficients given by relations (19) to (22). In order to do this, the wave matrix **H** was expressed as a product of wave matrices which relate waves at the midpoints of neighbouring uniform segments, as in references [5, 6]. The time histories of the reflected and transmitted waves at the gauge positions, corresponding to one of the measured incident waves for each transmission direction, were obtained by using FFT and considering the elastic bars between the gauges as parts of the junction.

In the simulations, PMMA was represented by a standard linear solid (parallel combination of spring E_1 and damper η in series with spring E_2). Thus, the complex modulus was expressed as

$$E(\omega) = E_2(E_1 + \mathrm{i}\omega\eta)/(E_1 + E_2 + \mathrm{i}\omega\eta). \tag{25}$$

The constitutive parameters were given the values $E_1 = 56{\cdot}6$ GPa, $E_2 = 5{\cdot}57$ GPa and $\eta = 2{\cdot}04$ MPas as obtained by Sakata *et al*. and reproduced by Sogabe & Tsuzuki [10]. The density of PMMA was taken to be $\rho = 1183\ \mathrm{kg/m^3}$. The Young's modulus and the density were taken to be $E = 70$ GPa and $\rho = 2700\ \mathrm{kg/m^3}$ for aluminium, and $E = 210$ GPa and $\rho = 7850\ \mathrm{kg/m^3}$ for steel, respectively.

4. RESULTS

Comparisons of experimental results for transmission directions A and B are made in Figures 6 and 7. Figure 6 shows the energy dissipation, reflection and transmission coefficients versus hammer length. The average values represented by each plotted point,

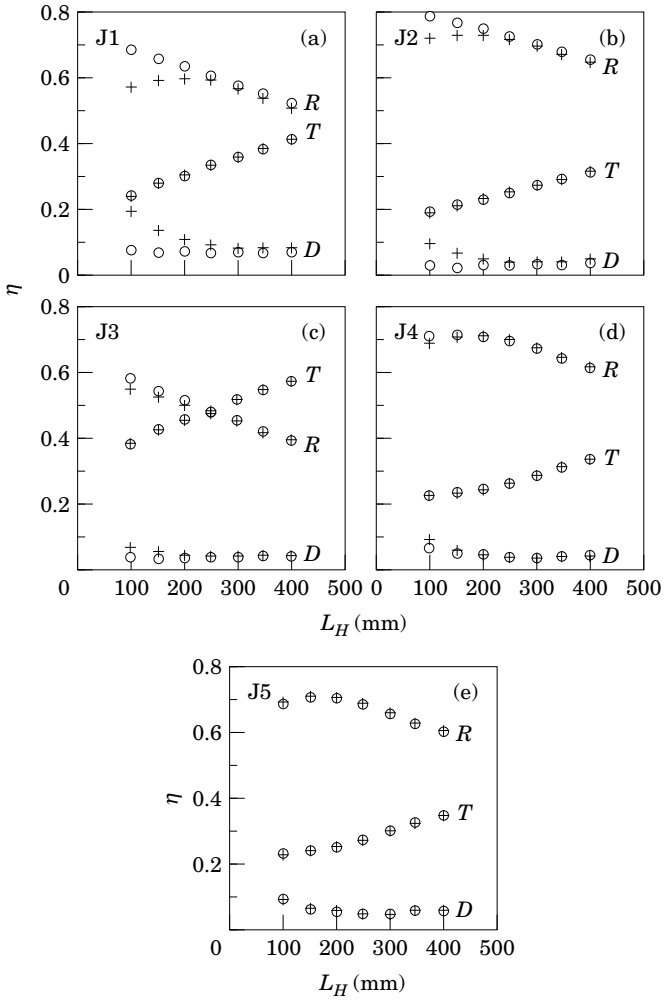

Figure 6. Energy dissipation (D), reflection (R) and transmission (T) coefficients η versus hammer length L_H for transmission directions A (○) and B (+). Experimental results for junctions (a) J1, (b) J2, (c) J3, (d) J4, and (e) J5.

and the corresponding standard deviations, are presented in tabular form in the Appendix. As predicted by theory, the dissipation and reflection coefficients are generally different for transmission directions A and B, while there is a close agreement between the corresponding transmission coefficients. Figure 7 shows strain histories (one from each series of five tests) associated with the incident, reflected and transmitted waves for the hammer length 250 mm. In agreement with theory, the reflected waves generally differ between transmission directions A and B, while there is close agreement between the corresponding transmitted waves.

Comparisons of results from experimental tests and numerical simulations are made in Figures 8 and 9. Figure 8 shows, for each transmission direction, the energy dissipation, reflection and transmission coefficients versus hammer length for the junction J3. Figure 9 shows corresponding strain histories associated with the incident, reflected and transmitted waves for the hammer length 250 mm. It can be seen that there is fair agreement between the results of experimental tests and numerical simulations.

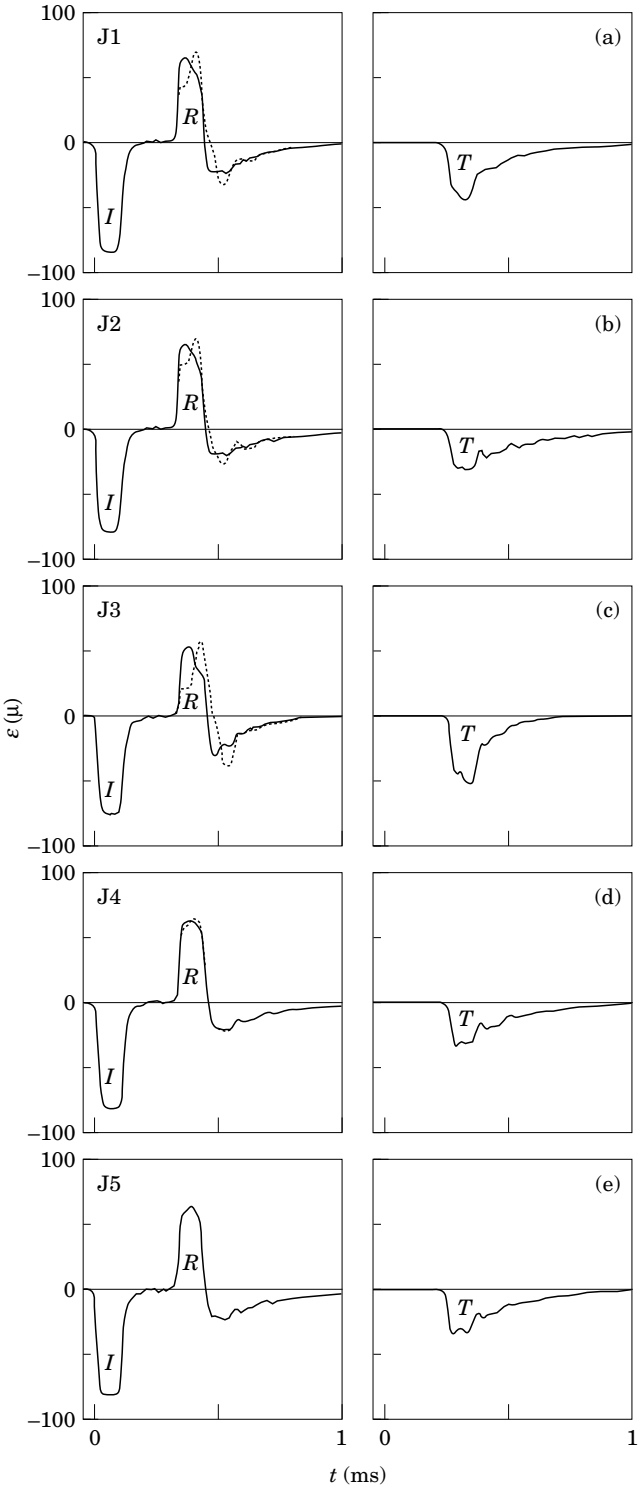

Figure 7. Strains ε associated with incident (I), reflected (R) and transmitted (T) waves versus time t for transmission directions A (solid curves) and B (dashed curves) with hammer length $L_H = 250$ mm. Experimental results for junctions (a) J1, (b) J2, (c) J3, (d) J4, and (e) J5.

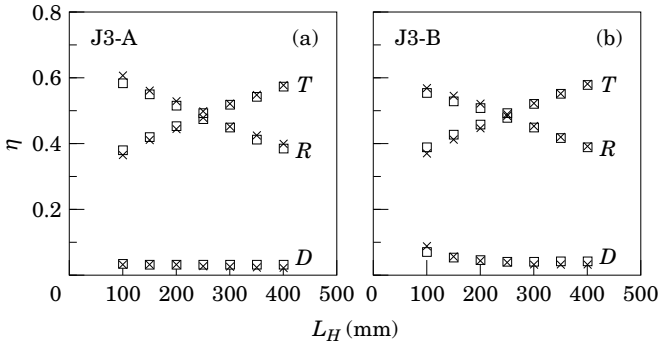

Figure 8. Energy dissipation (D), reflection (R) and transmission (T) coefficients η versus hammer length L_H for junction J3, made of PMMA and aluminium. Comparison of results from experimental tests ($\square$) and numerical simulations ($\times$) for transmission directions (a) A and (b) B.

5. DISCUSSION

The phenomena of dissipation, reflection, and transmission of waves and wave energy at a viscoelastic junction between elastic bars have been studied theoretically and experimentally.

The 1-D theoretical study, in which linear material behaviour is assumed, shows that the dissipated energy, and the reflected wave and its energy, generally depend on the transmission direction. In contrast, and as a manifestation of reciprocity, the transmitted wave and its energy do not depend on the transmission direction. In the special case of a symmetric junction, naturally, there is no directional dependence for dissipation, reflection or transmission. Furthermore, in the special case of an elastic junction, the

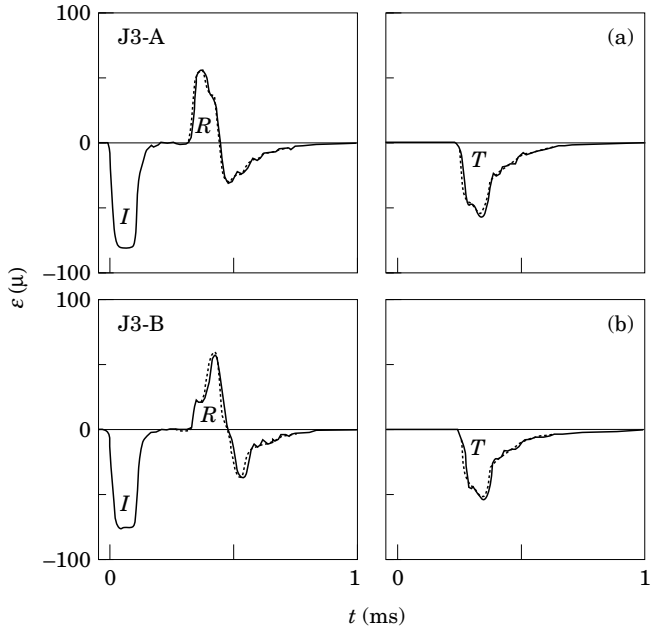

Figure 9. Strains ε associated with incident (I), reflected (R) and transmitted (T) waves versus time t for junction J3, made of PMMA and aluminium, and hammer length 250 mm. Comparison of results from experimental tests (solid curves) and numerical simulations (dashed curves) for transmission directions (a) A and (b) B.

dissipation is zero. Consequently, the dependence of the energy dissipation coefficient on the transmission direction can be expected to increase with the degrees to which a junction is non-symmetric and dissipative. If instead a 3-D model were to be used, it would be expected that the principal results obtained here with the 1-D model would remain valid.

The energy dissipation coefficients generally decrease with hammer length to almost constant values, while the energy reflection coefficients decrease with hammer length or have a maximum. The decrease in energy dissipation coefficient with hammer length may be interpreted in terms of the behaviour of the standard linear solid model, which has been seen to represent fairly well the material of junction J3 (PMMA). Thus, consider the response of the material when a junction is loaded by a rectangular incident wave. Clearly, the damper η and spring E_1 in parallel will deform, and dissipation will occur, mainly during one period after the rise and another after the fall of the incident wave. Between these dissipation periods, the strain of the viscoelastic material will be nearly constant and determined by the stress and the springs E_1 and E_2 in series. If the incident wave is short (duration comparable to the dissipation periods or less), then, dissipation will take place during the complete transmission and reflection process, and the energy dissipation coefficient will be relatively high. If, instead, the incident wave is long (duration much longer than the dissipation periods), dissipation will take place mainly at the beginning and end of the transmission and reflection process and the energy dissipation coefficient will be relatively low. For very long incident waves, the energy dissipation coefficient would tend to zero, while the observed behaviour is that it tends to a low but finite value. This may indicate a limitation of the standard linear solid model. Then, an improved representation of the constitutive behaviour might be obtained by adding a series damper to this model. For a very long incident wave, then, the strain rate would be determined by the stress and this damper during the major part of the transmission and reflection process, and this would make the dissipation coefficient nearly independent of the length of the incident wave. Another possibility is that for the longest incident waves, the integration intervals in equations (24) for the reflected and transmitted waves could not be chosen long enough because of disturbing reflections from the bar ends. This would lead to slight underestimations of the reflection and transmission coefficients, and corresponding, but possibly significant, overestimations of the dissipation coefficients according to equations (21) and (22).

For junctions J1 and J2 there are marked differences between the energy reflection coefficients, and between the energy dissipation coefficients, for the two transmission directions, especially for short hammers. For junction J1 and a hammer with length 100 mm, e.g., the energy dissipation coefficient is $0{\cdot}073 \pm 0{\cdot}004$ with transmission direction A and $0{\cdot}190 \pm 0{\cdot}003$ with transmission direction B. Thus, in this case the energy dissipation coefficient is 2·6 times larger in the second case than in the first. For junctions J3 and J4 the directional dependence of the energy reflection and dissipation coefficients is weaker. For junction J5, which is symmetric, there is close agreement between the energy dissipation coefficients, and between the energy reflection coefficients, for the two transmission directions. This is expected and may serve as a test for the accuracy of the measurements. For all junctions tested, the energy transmission coefficients increase with hammer length, and there is close agreement between these coefficients for the two transmission directions; see Figure 6 and the Appendix.

For the non-symmetric junctions J1 to J4, the energy dissipation coefficients are always the lowest with transmission direction A. A conceivable explanation can be found from a study of Figure 7, which shows how the reflected waves depend on the transmission direction. It can be seen that the reflected waves are always initially tensile. This is due

to the mis-match between the input bar, with relatively high characteristic impedance, and the first segments of each junction, which have relatively low magnitudes of their characteristic impedances. Furthermore, it can be seen that the initial tensile strain is always the largest with transmission direction A. Thus, the energy dissipation coefficient is the lowest for the transmission direction which gives the largest mis-match at the input end of a junction. For this transmission direction, clearly, there is the largest fraction of the incident wave energy which is reflected initially and which therefore cannot contribute to the dissipation in the junction. For junctions J1 to J3 this means that wave transmission occurs from the thinner to the thicker end of the junction.

ACKNOWLEDGMENT

The authors are indebted to the Swedish Research Council for Engineering Sciences (TFR) for financial support.

REFERENCES

1. M. Mao and D. Rader 1970 *International Journal of Solids and Structures* **6**, 519–538. Longitudinal pulse propagation in non-uniform elastic and viscoelastic bars.
2. S. E. Hanneman and V. K. Kinra 1992 *Experimental Mechanics* **32**, 323–331. A new technique for ultrasonic non-destructive evaluation of adhesive joints: Part I. Theory.
3. S. E. Hanneman, V. K. Kinra and C. Zhu 1992 *Experimental Mechanics* **32**, 332–339. A new technique for ultrasonic non-destructive evaluation of adhesive joints: Part II. Experiment.
4. B. Lundberg, R. Gupta and L.-E. Andersson 1979 *Wave Motion* **1**, 193–200. Optimum transmission of elastic waves through joints.
5. T. Nygren, L.-E. Andersson and B. Lundberg 1996 *European Journal of Mechanics A/Solids* **15**, 29–49. Optimum transmission of extensional waves through a non-uniform viscoelastic junction between elastic bars.
6. L.-E. Andersson and B. Lundberg 1984 *Wave Motion* **6**, 389–406. Some fundamental transmission properties of impedance transitions.
7. B. R. Mace 1992 *Journal of Sound and Vibration* **155**, 375–381. Reciprocity, conservation of energy and some properties of reflection and transmission coefficients.
8. J. F. Allard, B. Brouard, D. Lafarge and W. Lauriks 1993 *Wave Motion* **17**, 329–335, Reciprocity and antireciprocity in sound transmission through layered materials including elastic and porous media.
9. E. A. Coddington and N. Levinson 1955 *Theory of ordinary differential equations*. New York: McGraw-Hill.
10. Y. Sogabe and M. Tsuzuki 1986 *Bulletin of the Japan Society of Mechanical Engineers* **29**, 2410–2417. Identification of linear viscoelastic materials by the wave propagation testing.

APPENDIX

The average values for the energy reflection, transmission and dissipation coefficients obtained in the experimental tests, and the corresponding standard deviations, are given in Table A1.

(Table A1 overleaf)

TABLE A1

Average values and standard deviations for energy dissipation (D), reflection (R) and transmission (T) coefficients η obtained in experimental tests with transmission directions A and B for different hammer lengths L_H

Junction	L_H (mm)	η_D^A (10^{-3})	η_D^B (10^{-3})	η_R^A (10^{-3})	η_R^B (10^{-3})	η_T^A (10^{-3})	η_T^B (10^{-3})
J1	100	73 ± 4	190 ± 3	682 ± 2	569 ± 2	245 ± 2	241 ± 2
	150	67 ± 3	132 ± 3	655 ± 2	591 ± 2	278 ± 1	278 ± 1
	200	68 ± 2	106 ± 3	634 ± 2	595 ± 1	298 ± 1	299 ± 2
	250	66 ± 3	85 ± 2	605 ± 2	589 ± 1	329 ± 3	326 ± 1
	300	68 ± 3	81 ± 2	576 ± 2	563 ± 1	356 ± 1	356 ± 2
	350	67 ± 1	85 ± 2	551 ± 1	534 ± 0	383 ± 1	381 ± 2
	400	68 ± 2	85 ± 1	522 ± 1	506 ± 0	410 ± 2	409 ± 1
J2	100	23 ± 1	95 ± 3	784 ± 1	717 ± 3	193 ± 1	188 ± 2
	150	21 ± 3	66 ± 4	765 ± 2	724 ± 3	214 ± 1	210 ± 2
	200	26 ± 3	49 ± 3	746 ± 2	725 ± 2	227 ± 1	226 ± 2
	250	27 ± 1	40 ± 2	724 ± 1	714 ± 2	249 ± 1	246 ± 1
	300	29 ± 4	37 ± 1	701 ± 2	695 ± 1	270 ± 2	268 ± 1
	350	29 ± 4	42 ± 2	680 ± 2	668 ± 2	292 ± 2	290 ± 1
	400	35 ± 2	50 ± 1	653 ± 2	638 ± 1	312 ± 1	312 ± 0
J3	100	34 ± 3	65 ± 4	584 ± 2	550 ± 2	382 ± 1	384 ± 3
	150	31 ± 2	51 ± 3	548 ± 2	525 ± 0	422 ± 2	424 ± 2
	200	32 ± 2	43 ± 2	514 ± 1	503 ± 1	454 ± 2	455 ± 1
	250	33 ± 1	40 ± 1	480 ± 1	474 ± 1	487 ± 1	486 ± 0
	300	35 ± 1	38 ± 1	447 ± 1	445 ± 1	518 ± 1	517 ± 1
	350	38 ± 1	42 ± 1	417 ± 1	412 ± 1	545 ± 1	546 ± 1
	400	39 ± 1	42 ± 1	388 ± 1	386 ± 1	573 ± 1	571 ± 1
J4	100	70 ± 1	91 ± 2	706 ± 1	685 ± 2	224 ± 1	224 ± 1
	150	52 ± 4	60 ± 4	713 ± 3	706 ± 3	235 ± 2	234 ± 1
	200	48 ± 3	49 ± 3	708 ± 3	708 ± 2	244 ± 2	243 ± 2
	250	41 ± 3	39 ± 2	695 ± 3	698 ± 1	264 ± 2	263 ± 1
	300	39 ± 3	39 ± 4	674 ± 2	674 ± 2	288 ± 2	287 ± 2
	350	43 ± 2	44 ± 3	645 ± 1	644 ± 2	312 ± 2	313 ± 1
	400	47 ± 3	47 ± 3	616 ± 2	616 ± 1	337 ± 1	337 ± 2
J5	100	92 ± 2	88 ± 2	681 ± 2	685 ± 2	228 ± 1	227 ± 3
	150	58 ± 4	61 ± 2	702 ± 2	702 ± 2	240 ± 2	236 ± 1
	200	52 ± 2	54 ± 3	699 ± 1	699 ± 3	249 ± 1	247 ± 1
	250	47 ± 2	45 ± 2	681 ± 2	683 ± 2	273 ± 0	272 ± 1
	300	46 ± 3	48 ± 3	654 ± 2	654 ± 1	300 ± 2	298 ± 3
	350	52 ± 1	53 ± 2	623 ± 0	624 ± 2	326 ± 1	323 ± 1
	400	53 ± 2	50 ± 1	602 ± 2	603 ± 1	345 ± 1	347 ± 1